

# RSC Advances



This is an *Accepted Manuscript*, which has been through the Royal Society of Chemistry peer review process and has been accepted for publication.

*Accepted Manuscripts* are published online shortly after acceptance, before technical editing, formatting and proof reading. Using this free service, authors can make their results available to the community, in citable form, before we publish the edited article. This *Accepted Manuscript* will be replaced by the edited, formatted and paginated article as soon as this is available.

You can find more information about *Accepted Manuscripts* in the [Information for Authors](#).

Please note that technical editing may introduce minor changes to the text and/or graphics, which may alter content. The journal's standard [Terms & Conditions](#) and the [Ethical guidelines](#) still apply. In no event shall the Royal Society of Chemistry be held responsible for any errors or omissions in this *Accepted Manuscript* or any consequences arising from the use of any information it contains.

**Continuous Fast Fourier transform admittance voltammetry as a new approach for study  
the change morphology of polyaniline for supercapacitors application**

**J. Shabani Shayeh<sup>a</sup>, P. Norouzi<sup>\*a</sup>, M.R. Ganjali<sup>a</sup>, M. Wojdyla<sup>b</sup>, K.Fic<sup>b</sup>, E. Frackowiak<sup>b</sup>**

<sup>a</sup> Center of Excellence in Electrochemistry, University of Tehran, Tehran, Iran

<sup>b</sup> Poznan University of Technology, Institute of Chemistry and Technical Electrochemistry, Piotrowo 3, 60965 Poznan, Poland

\* Corresponding author. Tel.: +98 21 61112788; fax: +98 21 66495291. E-mail address: norouzi@khayam.ut.ac.ir (P. Norouzi).

## Abstract

In this work, Continuous Fast Fourier transform admittance voltammetry (CFFTAV) was used to study and characterization the surface morphology of polyaniline (PANI) on glassy carbon (GC) electrode. Four polymer films with various thicknesses (0.5  $\mu\text{m}$  to 11 $\mu\text{m}$ ) were synthesized by electrochemical method. A new modified square wave voltammetry (SWV) method based on application of discrete Fast Fourier Formation (FFT) method, background subtraction and two-dimensional integration of the electrode response over a selected potential range and time window was used. Also, the electrode response could be calculated by measuring the changes in SW voltammogram (or admittance). Results showed that by using CFFTAV method, changes in the porosity of PANI and the behavior of PANI formation in  $\text{H}_2\text{SO}_4$  solution were investigated more quantitative than, scanning electron microscopy (SEM), cyclic voltammetry (CV), charge-discharge (CD) and impedance spectroscopy (EIS) methods. By monitoring the electrode response, kinetic for reaching to the steady state condition was studied. It was found that, with increasing the thickness of polymer film from 0.5  $\mu\text{m}$  to 11 $\mu\text{m}$  the accessible porosity decrease by up to three times. Furthermore, dimensions of micro channels in the polymer film decreased with increasing the thickness. Also, maximum potential for ion insertion increased from 324 mV to 365mV. Capability of electrodes for using as supercapacitor materials were tested by CV, CD and EIS, and the calculated capacity of electrodes were equal to 620  $\text{Fg}^{-1}$  and 247  $\text{Fg}^{-1}$  for thinnest and thickest polymer film, respectively.

Keywords: Continuous FFT Admittance voltammetry, Polyaniline, Porosity, Supercapacitors.

## 1. Introduction

Supercapacitors (SCs) are modern energy storage systems, which nowadays get huge scientific interests due to their ability to deliver very high impulses of energy in a very short time, good cyclic efficiency, long cyclability and lack of environmental toxicity. SCs find applications in electric and hybrid cars and buses, wind turbines, UPC systems etc <sup>1-5</sup>. Conducting polymers (CPs) also called synthetic metals such as PANI, polypyrrole or polythiophene are promising electrode materials for SCs due to their good conductivity, good thermal and chemical stability, high doping effect and fast electrochemical switching<sup>6-8</sup>.

PANI is one of the popular electrode materials which has been used for SCs, because of its diverse structure, thermal and radiation stability, relatively low cost and easy synthesis <sup>9, 10</sup>. It can exhibit very high capacitance values, which can tend to even 1000 Fg<sup>-1</sup> per one electrode, when electrochemical research is conducted in three electrode cell with using a thin film of PANI <sup>11</sup>.

The main parameter of CPs, which specifies possibility of their application as electrode material in SCs is the porosity or the number of active sites, due to its critical influence on the capacitance of the CP electrode. Porosity or active site of various materials can be determined by using the following techniques: physical adsorption of gases, mercury porosimetry, small angle scattering (SAS), of neutrons (SANS) or X-rays (SAXS), transmission electron microscopy (TEM), scanning electron microscopy (SEM), scanning tunnel microscopy (STM), immersion calorimetry and etc <sup>12</sup>. Nevertheless, in the earlier publications for specifying the porosity of CPs, there is lack for a method for identifying the type porosity of the polymer film. The major techniques for study of the porosity cannot be used for thin polymer film, like adsorption of gases or mercury porosimetry. Additionally, some other methods, like TEM, SEM and other microscopy techniques, require film drying which changes the structure of the film<sup>13</sup>. As a result, investigation of CPs porosity gains problems and for solving these problems we suggest CFETA technique that is a new modified SWV method for study the surface of PANI film. Due to some unique features of SWV such as selectivity and sensitivity more than some ordinary method such as CV and EIS this electrochemical technique has various application like sensing and bio sensing materials which spanning various fields. Electrochemical sensor and biosensors<sup>14-17</sup>, environmental pollution<sup>18, 19</sup>, food science<sup>20, 21</sup> and enzyme kinetic<sup>22, 23</sup> are some

examples that illustrate application of SWV. In this work, continuous fast Fourier transform admittance voltammetry (CFFTAV) was used to study of characterization of the formed polyaniline film on glassy carbon (GC) electrode. At first, PANI films were synthesized by cyclic voltammetry technique on the surface of GC electrode and after that studied in H<sub>2</sub>SO<sub>4</sub> solution, with CFFTAV technique. After film formation, porosity and the types PANI were determined. For showing the capability of these electrodes to using in supercapacitor devices the property of electrode was tested by CV, CD and EIS technique.

## 2. Experimental

### 2.1 Materials and Morphological investigations and electrochemical evaluation

Aniline was vacuum-distilled at 120°C and stored in refrigerator before use. Analytical-grade reagents, were used as received without any pretreatment. Double-distilled water was used for the preparation of solutions. Morphological investigations of the polymeric films were carried out by using SEM (Philips XL 30).

Electrochemical experiments (CV, CD and EIS) were carried out by an Autolab General purpose System PGSTAT 30 (Eco-chime, Netherlands). A conventional three electrode cell containing a glassy carbon electrode with an area of 0.03 cm<sup>2</sup> as the working electrode, platinum wire as the counter electrode and an Ag/AgCl reference electrode (Argental, 3 M KCl) was used. The EIS experiments were conducted in the frequency range between 100 kHz and 10 mHz with a perturbation amplitude of 5 mV.

### 2.2 Synthesis of PANI

Electrochemical polymerization of PANI was done by using CV technique on GC electrode. Four different thickness of PANI was formed by applying 3, 5, 7 and 12 cycles which named PANI1, PANI2, PANI3 and PANI4 respectively, in potential range -0.2 to 1.2 V, at the scan rate of 50 mVs<sup>-1</sup> in solution of 0.03 M aniline in 1.0 M H<sub>2</sub>SO<sub>4</sub>. The mass of the PANI films was approximated assuming a current efficiency for the electropolymerization process of 100% using Faraday's law of electrolysis<sup>24</sup>.

### 2.3 Continues FFT admittance voltammetric measurements.

For the electrochemical CFFTAV measurements a homemade potentiostat that was connected to a PC was used. The potentiostat was connected with an analog to digital (A/D) data acquisition board (PCL-818H, Advantech Co.). The data acquisition board, also, was used for generating the analog waveform and acquiring current. The potential waveform was repeatedly applied to the working electrode and then the data was acquired, and stored by the software. In the measurements, the data acquisition requirements electrochemical software was developed using

Delphi 6.0. Also, in this electrochemical setup, the data could be processed and plotted in real time, or the stored data could be loaded and reanalyzed the voltammograms. In order to improve the detector sensitivity, the SWV technique was modified in the potential excitation waveform and current sampling and data processing. Fig. 1 shows the potential waveform used for the measurements. In the modified technique, the currents sampled four times per each SW polarization cycle, and the potential waveform contained one additional potential step,  $E_s$  for conditioning the electrode. As is shown in Fig. 1, the measurement part of the wave form contains multiple SW pulses cycles with a amplitude of  $E_{sw}$  and frequency of  $f_0$ , were superimposed on a staircase potential function, which was changed by a small potential step of  $\Delta E$ . The values of potential pulse of SW ( $E_{sw}$ ) and  $\Delta E$  were in a range of few mV (10 to 50 mV). In the computer program, the number of SW cycles,  $N_c$ , in each staircase potential step was calculated based on the SW frequency,

$$N_c = f_0 / 1400 \text{ Hz} \quad \text{for } f_0 > 1400 \text{ Hz} \quad (1)$$

and

$$N_c = 1 \quad \text{for } f_0 \leq 1400 \text{ Hz} \quad (2)$$

The values of  $N_c$ ,  $f_0$ ,  $E_{sw}$ ,  $E_{initial}$  and  $E_{final}$  were the variable parameters in the measurements. It should be noted that in this technique all electrochemical processes involve insertion of negative ions, hence both charging and faradic currents may potentially carry useful analytical information. To get such information, it was important to sample current at a frequency at least two times higher than the current transducer bandwidth. In order to fulfill this requirement the sampling frequency was set always between 40 and 70 kHz (depending on applied SW frequency). In addition, a second order low pass filter with a 20 kHz cutoff frequency was placed between the current output of the potentiostat and the data acquisition board. In this technique, modified SW voltammetry method based on application of discrete FFT method, background subtraction and two-dimensional integration of the electrode response over a selected potential range and time window. Also, the electrode response could be calculated by measuring the changes in SW voltammogram (or admittance)<sup>25-28</sup>. During FFT measurement, at first a positive ramp voltage from 0.2 to 0.6 V was applied to the electrode by the frequency of 2500 Hz and amplitude of 0.05 V.

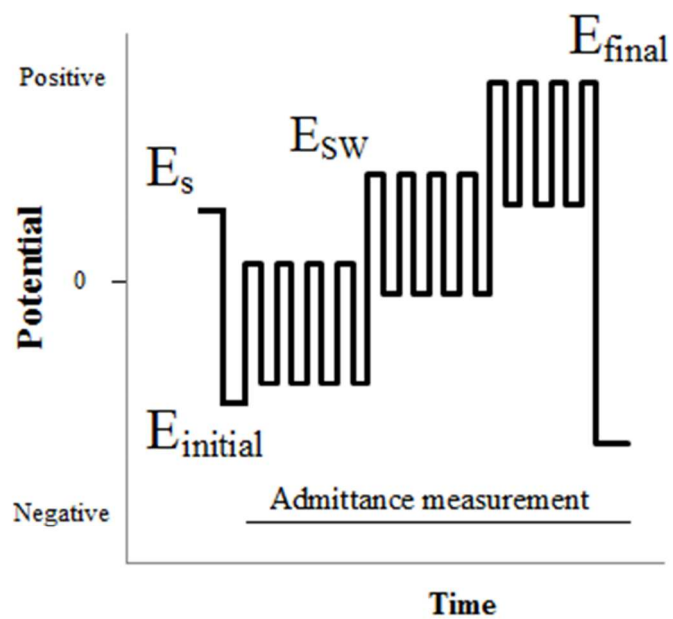


Fig. 1. Applied potential waveform during FFT measurement

### 3. Results and discussion

#### 3.1 Electrochemical measurements

Fig. 2 demonstrates CVs for electro polymerization of PANI4 electrode. As mentioned the procedure for synthesis of all electrodes is same and just the number of cycles for electropolymerization is the difference between the electrodes. As can be seen CVs for electro polymerization show three redox peaks. The first redox peak at 0.3 and -0.1 V is related to the formation of free radicals in the polymer chains, and the second peak at 0.5 and 0.4 V is attributed to oxidation and reduction of intermediate, that produced by degradation of products, and the third redox pair was related to oxidation of PANI<sup>29</sup>.

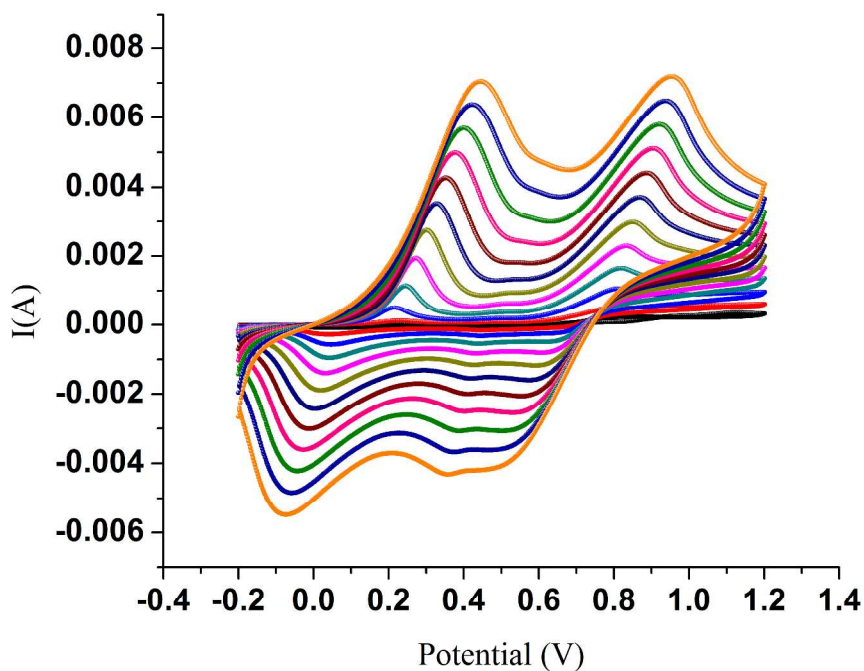


Fig. 2. Cyclic voltammograms for electropolymerization of polyaniline on the surface of GC electrode.

The thickness of the polymer ( $d$ ) was estimated from the charge  $Q_i$  necessary to switch from Leucoemeraldine (LE) to Emeraldine ( $EM^{2+}$ ) form of PANI according to the equation:

$$d = \frac{Q_i M_w}{Z A \rho F} \quad (1)$$

Where  $Q_i$  is the charge under the first cyclic voltammogram peak;  $M_w$  is the molecular weight of aniline;  $Z=0.5$  (number of electrons/aniline unit);  $A$  is the area of the electrode ( $0.0314 \text{ cm}^2$ );  $\rho$ ,

the specific density of aniline ( $1.02 \text{ g cm}^{-3}$ ); and  $F$  is the Faraday's constant. The method calculates the total quantity of PANI, without taking into account the porosity factor and counterion volume<sup>11</sup>. Table 1 shows the summaries the PANI electrodes used in this study.

Table 1. Charge ( $Q_i$ ) and thickness ( $d$ ) of PANI films.

Electrode	$Q_i(\text{mC})$	$d(\mu\text{m})$	Number of polymerization cycles
PANI1	0.86	0.5	3
PANI2	3.8	2.5	5
PANI3	7.5	4.5	7
PANI4	18.3	11	12

Fig. 3 presents the SEM graphs of four PANI electrodes. As can be seen by increasing the thickness of polymer films, surface morphology of electrodes changed and the free spaces between polymer filaments decreased. Entangling the polymer fibers together, increasing the surface of electrodes for electropolymerization of PANI caused to compaction of polymer fibers together and result to decreasing the useful space for insertion/ deinsertion of ions on PANI active sites. Although SEM graphs are benefit data for study the surface morphology of conductive polymers but these results are qualitative and for quantitative results we used CFFTA method.

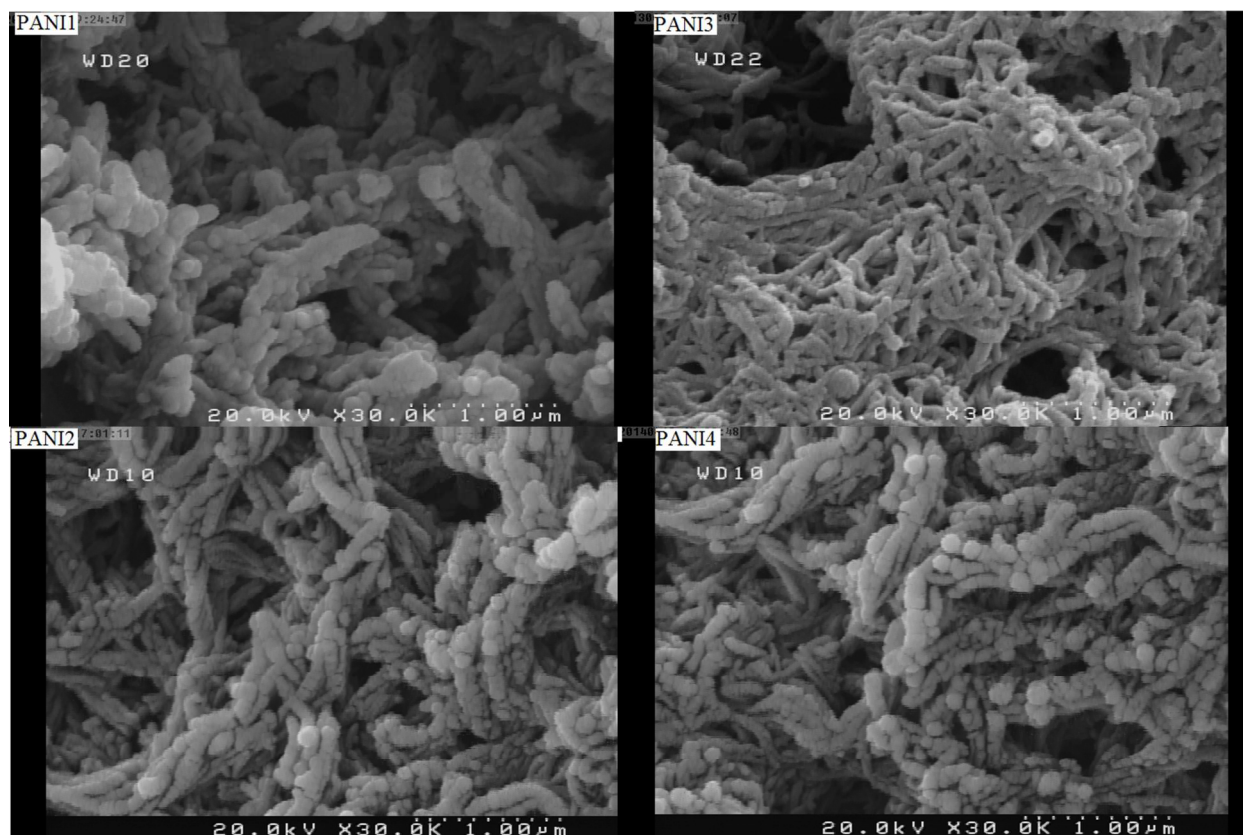


Fig. 3. SEM graphs of PANI electrodes.

Fig. 4 shows the (a) CVs of PANI electrodes at sweep rate of 25mV/s and (b) CD plots of four polymer films at current density of  $1.8 \text{ Ag}^{-1}$  in  $1.0 \text{ M H}_2\text{SO}_4$  media. As shown in the figure, in all CV curves a pair redox peaks related to the transition from Emeraldine to Pernigraniline form of PANI appear. With increasing the thickness of the polymer film that formed on the surface of GC electrode, the charging current of the CV curves (or charge Q) increased, which causes capacity of electrodes enhanced but, due to mass of the polymer, the specific capacitance of electrode diminished, significantly. The capacity of electrodes for PANI1, PANI2, PANI3, and PANI4 calculated  $620, 332, 288, 247 \text{ Fg}^{-1}$  respectively. According to formula,

$$C = \frac{Q}{V \times m} \quad (2)$$

Where V is the potential window and m is the mass of PANI<sup>30</sup>. Galvanostatic charge- discharge (GCD) measurement is a comprehensive technique for confirm the CV data of PANI electrodes. Fig. 4. b) Presents the CD plots of PANI electrodes at current density of  $1.8 \text{ Ag}^{-1}$  in  $1 \text{ M H}_2\text{SO}_4$

solution. Increasing the time needed to reach to cutoff potential by increasing the thickness of polymer film shows that the active sites of polymer films increased, but this active sites related to whole film body. It is well known that in low sweep rates, the ions in the solution have enough time for doping process to the polymer matrix.

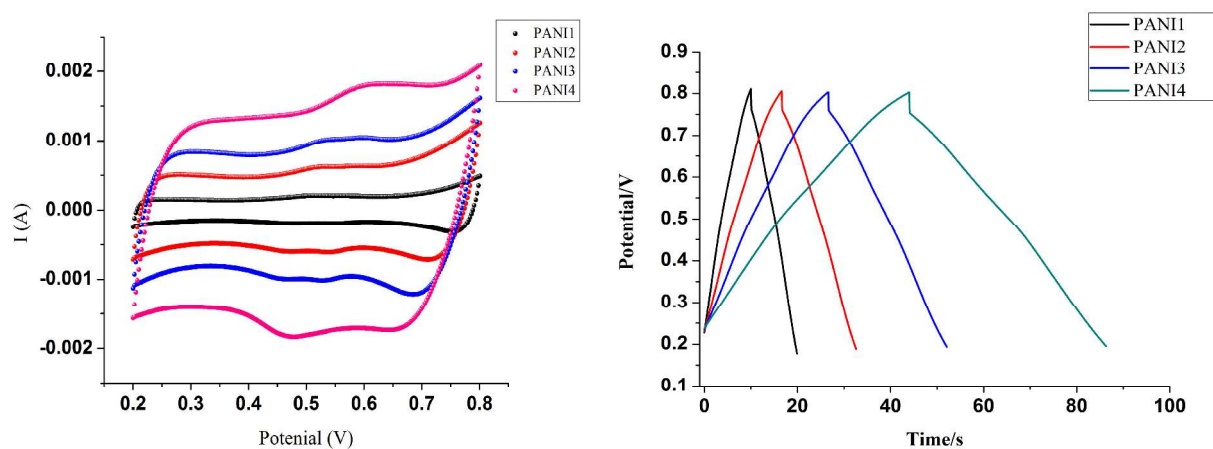


Fig. 4. a) CVs of PANI electrodes at sweep rate of 25mVs<sup>-1</sup>, b) CA plots of four polymer films at current density of 1.8 Ag<sup>-1</sup> in 1.0 M H<sub>2</sub>SO<sub>4</sub> solution.

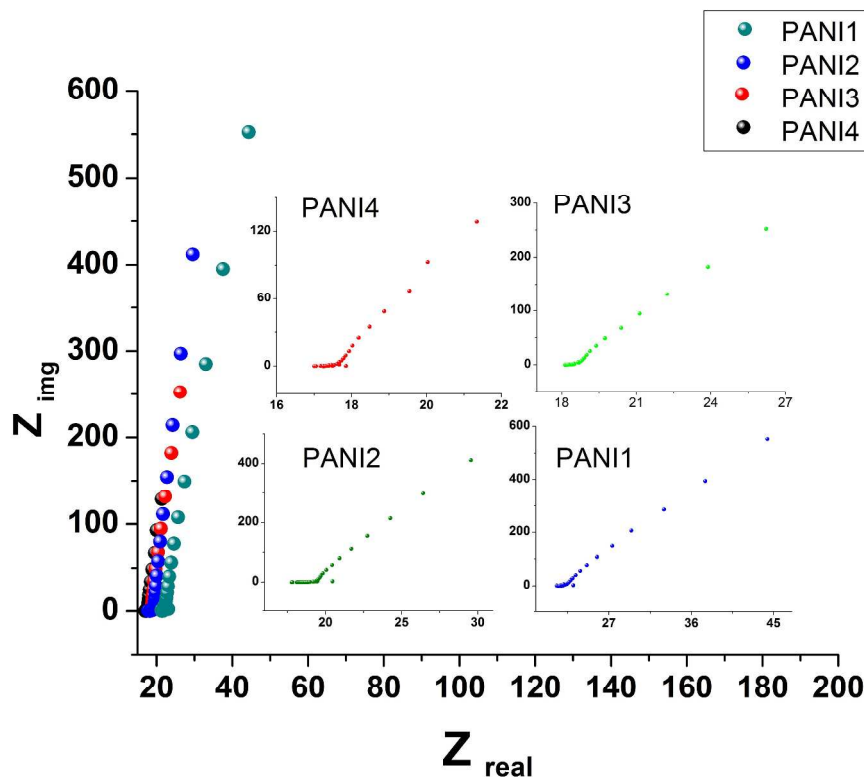


Fig. 5. Nyquist plots of the four electrodes in 1.0 M  $H_2SO_4$  solution.

Impedance spectroscopy is a suitable method for study the electrochemical features of CPs<sup>31,32</sup>. Fig. 5. shows the Nyquist plots of the electrodes in 1.0 M  $H_2SO_4$  solution. As shown in the figure, a semicircular loop in high frequency followed by a nearly vertical straight line in the low frequency is observed. The relationship between the imaginary impedance and capacitance of the model capacitor could be utilized to calculate the capacitance (at 10 mHz frequency),

$$C = \frac{1}{(2\pi f Z''')} \quad (3)$$

That  $f$  is the frequency and  $Z'''$  is the imaginary part of Nyquist diagram. The specific capacitance of the four electrodes were calculated 570, 290, 251, 190  $Fg^{-1}$  for PANI1, PANI2, PANI3 and PANI4 respectively. The value of calculated capacitance was slightly smaller than that obtained from cyclic voltammograms, but it shows that the specific capacitance calculated from cyclic voltammograms is reliable. Another feature of CPs for using as supercapacitors is their stability during continues cycles. Stability of four electrodes were tested using continues CVs and the results shows that by increasing the thickness of PANI electrodes from 0.5  $\mu m$  to 11  $\mu m$ , the stability of PANI electrodes enhanced from 30% to 50% after 800 continues cycles. The obtained CV, CD and EIS results confirmed that thicker films have more site or porosity but do

not provide information about the surface or beneath the surface of the polymer electrode. For study the reactions at the surface of polymer films we must use more higher scan rates. With the increasing the sweep rate the sensitivity of cyclic voltammetry method decreased and due to this phenomena CFFTAV method was used.

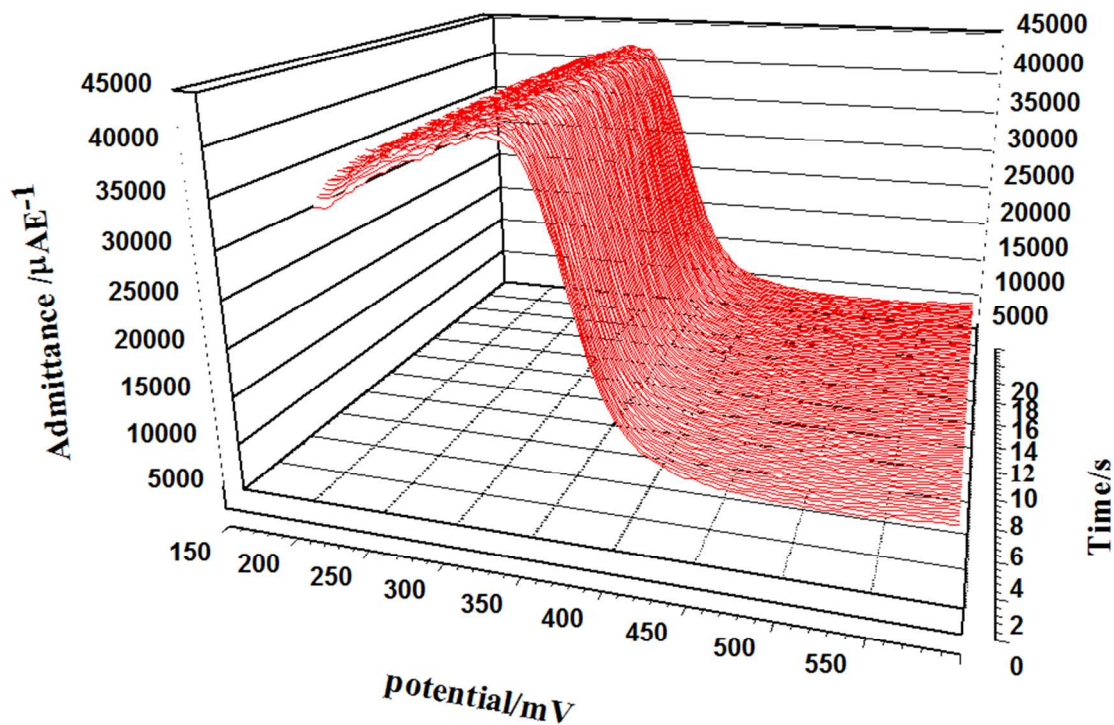


Fig. 6. 3D FFTAV graph of PANI1 electrode in 1.0 M H<sub>2</sub>SO<sub>4</sub> at the frequency of 2500Hz and amplitude 50 mV.

Fig. 6. Shows 3D plot of FFTA voltammograms for PANI1 electrode as a function of time in 1.0 M H<sub>2</sub>SO<sub>4</sub> at SW frequency of 2500Hz and amplitude 50 mV. At the potential of 0.2V polymer oxidizes to emeraldine form, which results to creation of positive charges on the electrode surface, that helps to insertion of negative ions into polymer matrix, the overall process is neutralization of the positive charges on the surface of the polymer. Therefore, by continuous application of potential waveform (in that time window), a large number of insertion and deinsertion of the ions in the polymer matrix occurred. Consequently, this ion exchange between solution and polymer film, produce a current or change the admittance of the electrode<sup>33-35</sup>.

It can be seen that during insertion of ions to polymer matrix, initially the admittance is growing due to the increasing amount of moving and accumulation of the ions, but when whole polymer matrix is full of ions, it is starting to decrease rapidly, to very low admittance level. After that the deinsertion process with strong impulse of negative voltage occurs ( $E_s$ ) then the next cycle is conducted. Using SW caused that ion rearranged during doping process and all the active sites fully used<sup>2, 26, 36</sup>. However, at high SW frequency, ions absorbed only on the surface of the polymer film and the inner section of the polymer have no ions absorption, due to insufficient time for ions to reach to that part. For the same reason, at high scan rate, only the surface of PANI film and beneath of surface, can be examined, which are the boundary active sites or porous on the electrode surface.

In order to see the details of changes in the admittance of electrodes at each potential, Differential admittance plots were used for various PANI samples, which are shown in Fig. 7. The background admittance was subtracted by this equation,

$$\Delta A_E = A_E - A_r \quad (3)$$

Where  $A_E$  is the value of admittance in the voltammogram, and  $A_r$  is the value of admittance in the reference voltammogram, which was recorded at the beginning of experiment. It can be seen, that by increasing the number of voltammogram, the admittance of the electrode was enhanced. It can be attributed to this fact that at the early cycles solvent molecules physically adsorbed and occupied some porosities of PANI films and by conducting the cycles these molecules removed from polymer matrix and the porosities can be useable. As shown, in 3D diagrams, reaching to a steady state for the polymer films occurs with different time scales. The value of admittance reaches the optimum value, after 7 seconds for PANI1 and 20 seconds for PANI4.

It can also be seen that when the polymer film is thicker, getting to the optimal value of admittance is longer and admittance of the polymers get smaller<sup>37</sup>. Additionally, in the admittance-potential-time curves, for PANI3 electrode some little noises appeared which have higher values for PANI4 electrode. Appearance of noise could be attributed to the fast replacement of the ions between active sites because of the proximity of the polymer chains that entangled together.

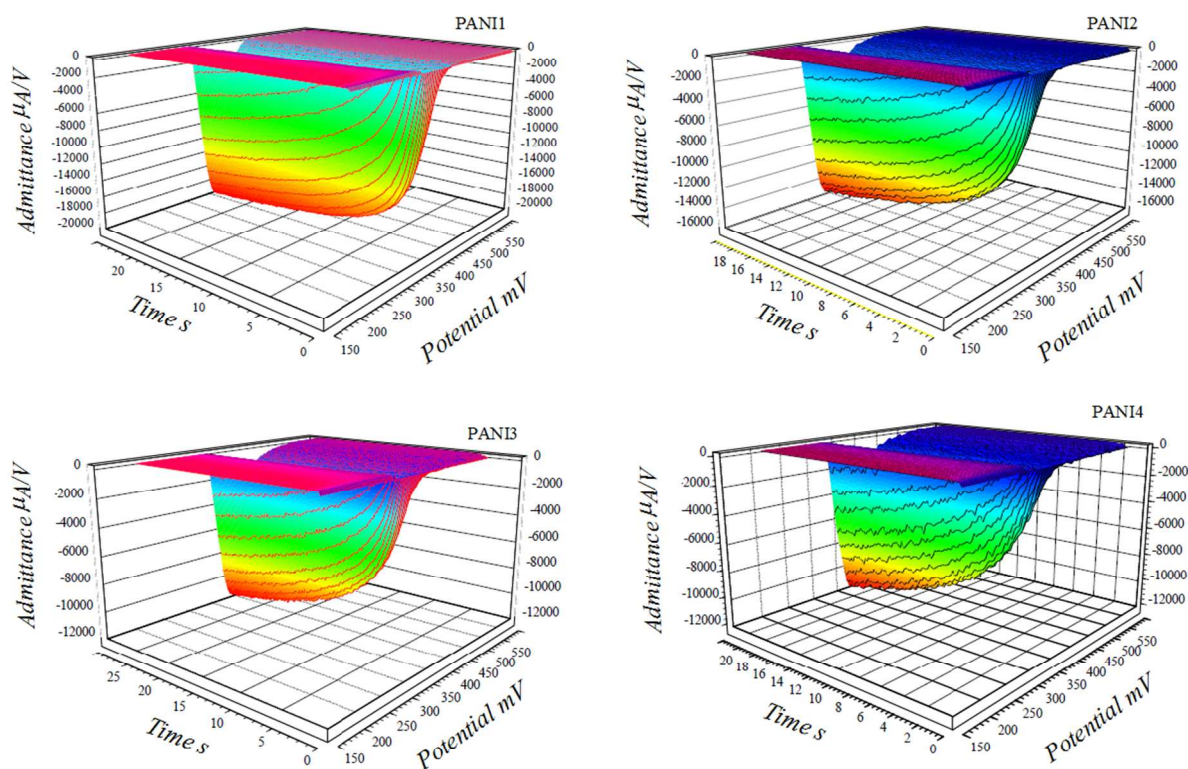


Fig. 7. 3D characterizations of differential admittance voltammogram to potential and time for PANI electrodes in 1.0 M H<sub>2</sub>SO<sub>4</sub> at the frequency of 2500 Hz and amplitude 50 mV.

By comparison PANI1 and PANI4, it can be seen that by increasing the thickness of polymer film the value of admittance of the electrodes decreased from 14877  $\mu\text{AV}^{-1}$  for PANI1 to 11018  $\mu\text{AV}^{-1}$  for PANI4 electrode. These phenomena occurred at high frequency and therefore only accessible porous were used. Therefore, by increasing the thickness of PANI the number of accessible porosity at the surface of PANI electrodes decreased. Thicker polymers also were checked and their behavior were the same and the magnitude of admittance decreased for thicker films. Furthermore the quantity of noise for thicker films increased. 2D plots of differential admittance – potential are presented in Fig. 8. From 2D differential admittance-potential curves the maximum potential for the insertion of ions into polymer matrix can be obtained. The horizontal plateau line is related to the first voltammogram that was saved as reference and subsequent voltammograms were subtracted from the reference voltammogram. All of these plots have three parts; the first part that has positive sign in potential range between 0.2 V to 0.3 V corresponds to oxidation of PANI and transformation to emeraldine form<sup>37</sup>. As polymer film

is oxidized and electrons are removed from electrode the mark of admittance is positive.

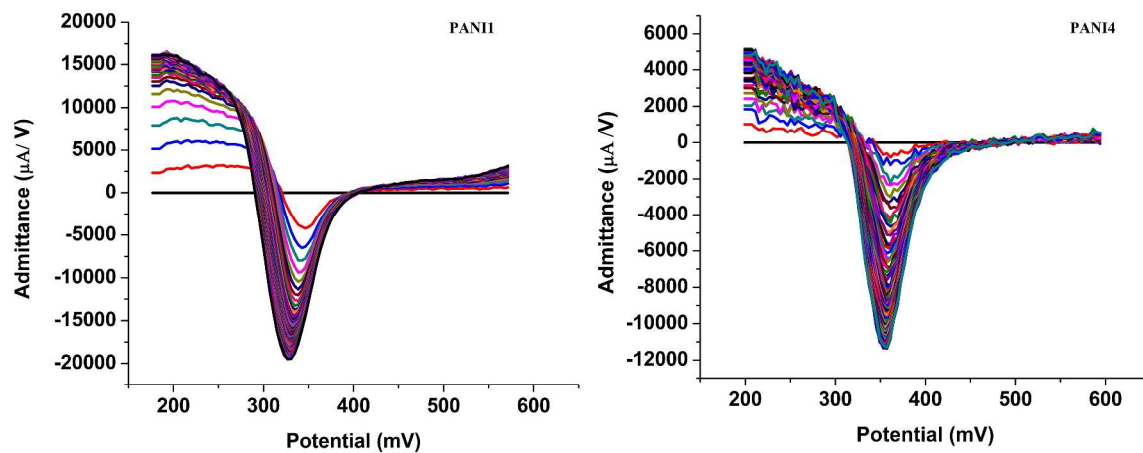


Fig. 8. 2D characterizations of differential admittance to potential for PANI electrodes in 1.0 M  $\text{H}_2\text{SO}_4$  at the frequency of 2500 Hz.

The second part (0.3 – 0.4V) relates to the insertion of ions to accessible porosity of polymer surface. As shown in fig 8, the potential of ion diffusion for PANI4 electrode is more than PANI1 film near to 41 mV. Thus, it could be suggested that for PANI4 electrode, the amount of the ion insertion in polymer matrix is lower than thinner films, so it is more difficult for ions to achieve to deeper porosities of the polymer matrix. This could be proving that PANI4 electrodes possesses higher amount of non accessible porosities than other electrodes in its surface or beneath the surface. Decreasing size of the micro-channel caused a higher peak potential, which is relate to diffusion of the ions into channels for doping process<sup>38, 39</sup>. This occurs because the ions are very close together and the repulsive forces between them cause to use more potentials for doping process. Third part of plots appears after the peak in 400 to 600 mV. This could be attributed to surface adsorption of the ions on the polymer film. The positive sign of admittance was related to surface adsorption of the ions on the polymer film surface. In this section, after insertion of the ions into the film polymer on the surface, an electrical double layer formed. Table 2 shows the obtained results for all electrodes.

Table 2. Results obtained all of the electrodes.

electrode	Maximum potential for insertion (mV)	Time of optimization (s)	Magnitude of Admittance $\mu\text{AV}^{-1}$
PANI1	324	7	19877
PANI2	334	11	12940
PANI3	353	16	11167
PANI4	365	20	11018

### 3.2 Effect of dilution.

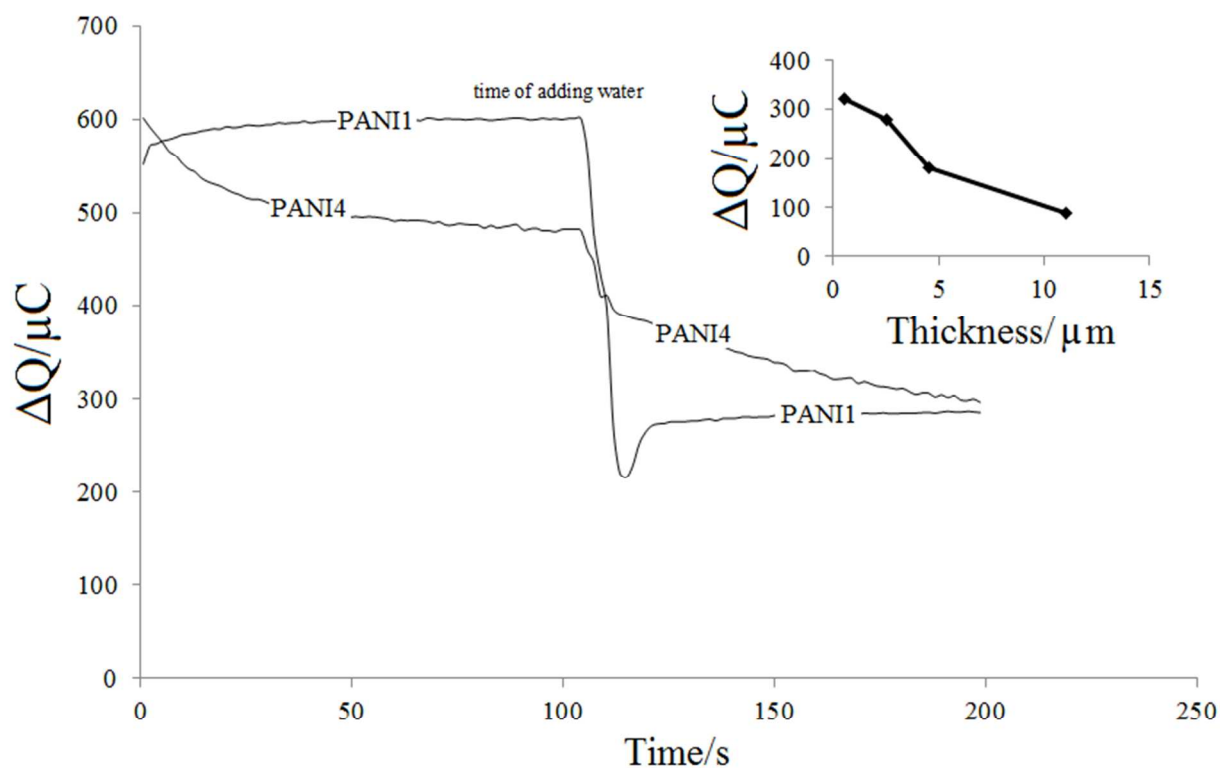


Fig. 9a) Response of the PANI electrodes to injection of water in 1.0 M  $\text{H}_2\text{SO}_4$  at the frequency of 2500 Hz and amplitude 50, b) plot of charge differences after adding water for all electrodes.

The calculation for the electrode response is based on integration of admittance in a selected potential range after background subtraction. The result of such calculation is the charge changes,  $\Delta Q$ , to obtain the signal of the polymer film oxidation and reduction. This can be obtained by using the following equation:

$$\Delta Q(s\tau) \sum_{E=E_i}^{E=E_f} (A(S, E)E - A(S_r, E)) \Delta t \quad (4)$$

Where,  $A(s, E)$  is the measured admittance of the PANI response at potential  $E$ , during the  $s$ -th sweep and  $A(s_r, E)$  is the reference admittance data of the PANI at potential  $E$ . The reference was obtained by saving of the first PANI CFFVA voltammogram in 1.0 M  $H_2SO_4$  solution at the frequency of 2500 Hz and amplitude 50 mV, which was used for background subtraction calculations is the sweep number,  $\tau$  is the time period between subsequent sweeps,  $\Delta t$  is the time difference between two subsequent admittance points at the voltammogram,  $E_i$  and  $E_f$  are initial and final of the potential integration, respectively.

Fig. 9 (main figure) shows the admittance–time plots of PANI samples. At the first of experiment the magnitude of polymer admittance plots as function of time in 1M  $H_2SO_4$  and then, after 100 seconds, water was added to the electrochemical cell to get half the concentration of ions. As shown in the figure, adding water to the reactor during the admittance measurement of PANI1 caused to destabilization of the system and large decrease of admittance, because of decreasing the amount of the ions, which disables occupation of some porosity. Nevertheless, when adding water to PANI4 electrode system, small effect is seen, therefore, it could be concluded, that in the PANI4 electrode the amount of accessible porosity or accessible active sites is low and after adding water the proportion of number of ions to the accessible porosities changes very small, compare to PANI1 electrode. Thus, in case of PANI4 electrode most of the porosities is not accessible for the ions and consequently the admittance is independent on the electrolyte concentration. Fig. 9 (inset figure) shows the plot of charge differences after adding water for all electrodes. As illustrated, by increasing the thickness of polymer film from  $0.5\mu m$  to  $11\mu m$ , the recorded charge decreased more than three times. Its resulted that the magnitude of active sites for PANI4 electrode is 3 times less than PANI1 electrode and the micro channels of thin film have more active sites for absorption of the ions compare with thicker one.

## Conclusions

CFETA technique is a promising tool for study the changes in the porosity of PANI and the behavior of PANI formation in  $H_2SO_4$  solution. Research revealed that using differential admittance analysis, it is possible to observe how the ions interact with polymer film during measurements and compare the quantity of active sites that exists in polymer film. Results that obtained by this method showed that by increasing the thickness of PANI film the size of micro channels and the number of active sites in PANI film decreased. By this method some parameter of polymer electrodes such as maximum potential of ion insertion and times needed for reaching to steady state ion exchange for the PANI electrodes was studied. It can have an estimation of accessible porosity based on the film thickness of the PANI, for example non accessible sites for PANI4 electrode is more three times than thin film polymer as PANI1 electrode

## Acknowledgement:

The financial support provided by the Research Council of the University of Tehran is gratefully appreciated.

## References

1. K. Jurewicz, S. Delpoux, V. Bertagna, F. Beguin and E. Frackowiak, *Chemical Physics Letters*, 2001, **347**, 36-40.
2. R. Kötz and M. Carlen, *Electrochimica Acta*, 2000, **45**, 2483-2498.
3. F.-J. Liu, *Journal of Power Sources*, 2008, **182**, 383-388.
4. A. Ehsani, A. Vaziri-Rad, F. Babaei and H. M. Shiri, *Electrochimica Acta*, 2015, **159**, 140-148.
5. A. Ehsani, *Progress in Organic Coatings*, 2015, **78**, 133-139.
6. Z. Niu, Z. Yang, Z. Hu, Y. Lu and C. C. Han, *Advanced Functional Materials*, 2003, **13**, 949-954.
7. R. Partch, S. Gangolli, D. Owen, C. Ljungqvist and E. Matijevec, 1992.
8. M. E. Roberts, D. R. Wheeler, B. B. McKenzie and B. C. Bunker, *Journal of Materials Chemistry*, 2009, **19**, 6977-6979.
9. J. Shabani-Shayeh, A. Ehsani, M. Ganjali, P. Norouzi and B. Jaleh, *Applied Surface Science*, 2015.
10. J. Shabani Shayeh, P. Norouzi and M. R. Ganjali, *RSC Advances*, 2015, **5**, 20446-20452.
11. L. Duić and S. Grigić, *Electrochimica acta*, 2001, **46**, 2795-2803.
12. E. Frackowiak, V. Khomenko, K. Jurewicz, K. Lota and F. Beguin, *Journal of Power Sources*, 2006, **153**, 413-418.
13. M. Ates, *Progress in Organic Coatings*, 2011, **71**, 1-10.
14. R. N. Goyal, S. Chatterjee, A. R. S. Rana and H. Chasta, *Sensors and Actuators B: Chemical*, 2011, **156**, 198-203.
15. K. Omidfar, A. Dehdast, H. Zarei, B. K. Sourkahi and B. Larijani, *Biosensors and Bioelectronics*, 2011, **26**, 4177-4183.
16. E. V. Suprun, A. A. Saveliev, G. A. Evtugyn, A. V. Lisitsa, T. V. Bulko, V. V. Shumyantseva and A. I. Archakov, *Biosensors and Bioelectronics*, 2012, **33**, 158-164.
17. S. Viswanathan, C. Rani, A. V. Anand and J.-a. A. Ho, *Biosensors and Bioelectronics*, 2009, **24**, 1984-1989.
18. R. O. Kadara, N. Jenkinson and C. E. Banks, *Electroanalysis*, 2009, **21**, 2410-2414.
19. A. Chen and B. Shah, *Analytical Methods*, 2013, **5**, 2158-2173.
20. S. M. Ghoreishi, M. Behpour and M. Golestaneh, *Analytical methods*, 2011, **3**, 2842-2847.
21. R. A. Medeiros, B. C. Lourencao, R. C. Rocha-Filho and O. Fatibello-Filho, *Analytical chemistry*, 2010, **82**, 8658-8663.
22. V. Shumyantseva, T. Bulko, A. Y. Misharin and A. Archakov, *Biochemistry*

- (Moscow) *Supplement Series B: Biomedical Chemistry*, 2011, **5**, 55-59.
23. S. Martić, M. Labib and H.-B. Kraatz, *Electrochimica Acta*, 2011, **56**, 10676-10682.
  24. N. Plesu, A. Kellenberger, M. Mihali and N. Vaszilcsin, *Journal of Non-Crystalline Solids*, 2010, **356**, 1081-1088.
  25. B. Ebrahimi, S. A. Shojaosadati, P. Daneshgar, P. Norouzi and S. M. Mousavi, *Analytica chimica acta*, 2011, **687**, 168-176.
  26. P. Norouzi, V. K. Gupta, F. Faridbod, M. Pirali-Hamedani, B. Larijani and M. R. Ganjali, *Analytical chemistry*, 2011, **83**, 1564-1570.
  27. P. Norouzi, B. Larijani, M. Ganjali and F. Faridbod, *Int J Electrochem Sci*, 2012, **7**, 10414-10426.
  28. P. Norouzi, B. Larijani, M. Ganjali and F. Faridbod, *Int. J. Electrochem. Sci*, 2014, **9**, 3130-3143.
  29. D. E. Stilwell and S. M. Park, *Journal of the Electrochemical Society*, 1988, **135**, 2254-2262.
  30. J. F. Mike and J. L. Lutkenhaus, *Journal of Polymer Science Part B: Polymer Physics*, 2013, **51**, 468-480.
  31. A. Ehsani, M. G. Mahjani, R. Moshrefi, H. Mostaanzadeh and J. S. Shayeh, *RSC Advances*, 2014, **4**, 20031-20037.
  32. J. Shabani-Shayeh, A. Ehsani and M. Jafarian, *Journal of the Korean Electrochemical Society*, 2014, **17**, 179-186.
  33. A. Ehsani, M. G. Mahjani, F. Babaei and H. Mostaanzadeh, *RSC Advances*, 2015, **5**, 30394-30404.
  34. F. Fusalba, P. Gouérec, D. Villers and D. Bélanger, *Journal of the Electrochemical Society*, 2001, **148**, A1-A6.
  35. Z. H. Zhou, N. C. Cai, Y. Zeng and Y. H. Zhou, *Chinese Journal of Chemistry*, 2006, **24**, 13-16.
  36. B. Zheng, Y. Zhao, W. Xue and H. Liu, *Surface and Coatings Technology*, 2013, **216**, 100-105.
  37. V. K. Gupta, P. Norouzi, H. Ganjali, F. Faridbod and M. Ganjali, *Electrochimica Acta*, 2013, **100**, 29-34.
  38. G. A. Snook, P. Kao and A. S. Best, *Journal of Power Sources*, 2011, **196**, 1-12.
  39. A. Karatrantos, R. J. Composto, K. I. Winey and N. Clarke, *Macromolecules*, 2011, **44**, 9830-9838.